Free Energy Calculations on the Binding of Colchicine and Its Derivatives with the α/β-Tubulin Isoforms

Jonathan Y. Mane and Mariusz Klobukowski*

Department of Chemistry, University of Alberta, Edmonton, Alberta, Canada T6G 2G2

J. Torin Huzil and Jack Tuszynski*

Division of Experimental Oncology, Cross Cancer Institute, Edmonton, Alberta, Canada T6G 1Z2

Received February 14, 2008

Tubulin is the target for numerous small molecule ligands which alter microtubule dynamics leading to cell cycle arrest and apoptosis. Many of these ligands are currently used clinically for the treatment of several types of cancer, and they bind to one of three distinct binding sites within β-tubulin (paclitaxel, vinca, and colchicine), all of which have been identified crystallographically. Unfortunately, serious side effects always accompany chemotherapy since these drugs bind to tubulin indiscriminately, leading to the death of both cancerous and healthy cells. However, the existence and distribution of divergent tubulin isoforms provide a platform upon which we may build novel chemotherapeutic drugs that can differentiate between different cell types and therefore reduce undesirable side effects. We report results of computational analysis that aims at predicting differences between the binding energies of a family of colchicine derivatives against 10 human α/β-tubulin isoforms. Free energy perturbation method has been used in our calculations and the results provide a proof of principle by indicating significant differences both among the derivatives and between tubulin isoforms.

1. INTRODUCTION

Microtubules are filamentous intracellular structures in all eukaryotic cells that are responsible for moving vesicles, granules, organelles like mitochondria, and chromosomes. They are important in mitosis or nuclear cell division, organization of intracellular structure, and intracellular transport, as well as ciliary and flagellar motility. A microtubule is a hollow filament of about 24 nm in diameter and is formed via polymerizations of the α/β-tubulin heterodimer. Since cancer cells divide much more rapidly than normal cells, a search for inhibitor drugs that would prevent cell division is of great importance.

During mitosis, microtubules construct the mitotic spindle, which is responsible for the segregation of aligned chromosomes prior to cell division. As such, microtubules have become the target for a large number of antimitotic agents including antitumor drugs such as the taxanes, epothilones, colchicine, and vinca alkaloids. The method of action of these drugs is to promote or inhibit microtubule polymerization by binding at specific sites on the interface of α/β-tubulin heterodimers. For example, the vinca alkaloid, vinblastine, binds at the intertubulin dimer interface, ultimately resulting in microtubule depolymerization.[1] On the other hand, binding of the taxanes results in an overall increase in the spindle microtubule mass with a concurrent reduction in microtubule dynamics.[2,3] The resulting cellular phenotype of these drugs is the induction of mitotic arrest leading to apoptosis, making them effective chemotherapeutic agents for targeting rapidly dividing cells. Nevertheless, even the most successful chemotherapy drugs have undesirable side effects that limit their utility. Their drawback is that when these drugs are given systemically, they bind tubulin indiscriminately, leading to the destruction of both cancerous and healthy cells, the consequence of which is the presence of serious side effects in all known cancer chemotherapy applications.

Colchicine is an antimitotic agent that has been considered for chemotherapy applications but is still in preclinical cancer research due to its toxicity. It suppresses cell division by inhibiting division of the cell's nucleus. Colchicine binds to the tubulin heterodimer and prevents tubulin from polymerization to form microtubules. Additionally, at high concentration, colchicine destabilizes the microtubule by inducing depolymerization. However, colchicine in its standard form has a fairly narrow range of effectiveness as a chemotherapy agent and is approved by FDA to treat gout. Colchicine would have to be administered in large doses to be effective in killing cancer cells. In doing so, however, it would not only kill the cancer cells but also many of the normal ones, leading to severe adverse events on patient. Thus, it would be prudent to find a substitute for colchicine as potential anticancer drugs that can be administered with reduced side effects for patients.

In this paper, we present a brief description of the tubulin isoforms, their 3-dimensional models, and the colchicine binding site. Our purpose in this study is to employ computational modeling in order to find derivatives of colchicine as potential anticancer drug candidates which would fit in the colchicine binding site of the α/β-tubulin

* Corresponding authors. E-mail: mariusz.klobukowski@ualberta.ca; phone: +1-780-492-3170; fax: +1-780-492-8231 (M.K.). Phone: +1-780-432-8906; fax: +1-780-432-8892 (J.T.).

10.1021/ci800054n CCC: $40.75
Published on Web 08/20/2008

Table 1. Tissue Distribution of β-Tubulin Isoforms in Normal Cells

isoform	organ expression	cellular expression
βI	constitutive	most cells
βII	brain, nerves, muscle; rare elsewhere	restricted to particular cell types
βIII	brain	neurons only
	testis	sertoli cells
	colon (very slight amounts)	epithelial cells only
βIVa	brain only	neurons and glia
βIVb	constitutive (not as widespread as βI)	high in ciliated cells, lower in others
βV	unknown	unknown
βVI	blood, bone marrow, spleen	erythroid cells, platelets
βVII	brain	unknown

heterodimer. To this end, we performed a series of free energy perturbation calculations[4−6] on the colchicine bound to several α/β-tubulin isoforms as well as on a number of derivatives of colchicine also bound to the same set of α/β-tubulin isoforms to elucidate which of these molecules may be considered to be potential substitute(s) for colchicine as an anticancer drug.

2. TUBULIN ISOFORMS AND THEIR 3D MODELS

Homologous protein families, such as tubulin, are collectively known as isoforms and have amino acid sequences that diverged as a result of accumulated mutations since their separation by speciation events.[7] The resulting variations in sequence can be neutral (when they are irrelevant to the process of natural selection) or essential (when they adapt the function of a protein to a given selective pressure).

At the molecular level, the role of tubulin is extremely complex and seems to be related to structural variations observed between α- and β-isoforms.[8] The existence and distribution of tubulin isoforms provide a link to their structure and their role in the polymerization and stability of microtubules. It is clear that much of the tubulin's surface is invariant; however, those substitutions that do occur are clustered at positions that comprise the longitudinal interface between protofilaments.[9] This observation implies that there must be a contribution from the interdimer interface, between protofilaments, that is key to our understanding of the properties that each isoform contributes to microtubule stability.

Isoform composition has previously been recognized as having a demonstrable effect on microtubule assembly kinetics[10,11] whereby small differences in the binding energies and chemical affinities of different tubulin isoforms surprisingly translate into significant deviations in the growth rates and catastrophe frequencies. Short-range interactions have been studied by calculating the energy of protofilament−protofilament interactions.[12]

Cells, especially cancer cells, are capable of altering the expression of each tubulin isoform (encoded by different genes) in response to external conditions that affect microtubule stability. There are several examples of this response; the most recent is the overexpression of β-tubulin isoform III (βIII) following exposure to microtubule stabilizing agents such as paclitaxel.[13−16] Table 1 identifies the distribution of β-tubulin isoforms in normal human cells. Current antitubulin drugs bind to all of these isoforms, having only slight preference for one over another.[17,18] For example, the vinca alkaloids bind best to βII,[17] providing an explanation as to their efficacy in leukemia and Hodgkin's lymphoma, since these cancerous cells express βII while normal lymphocytes do not.[19] We wish to stress that cancerous cells seem to express a variety of tubulin isoforms and are not limited to those expressed in the noncancerous cells from which they are derived.[20] Therefore, a drug that is highly specific for an isoform that is found within a cancerous cell could preferentially affect only those cells, while not harming significantly noncancerous cells.

To examine the molecular properties of tubulin isoforms and the effect that they have on microtubule dynamics and drug interactions, we earlier[9] performed a search of both the SWISS-PROT and Entrez protein databases.[21] We identified a total of seven human α-tubulin isoforms and eight β-tubulin isoforms. Following the identification of 83 individual protein sequences, corresponding only to β-tubulin, a ClustalW alignment was performed.[22] The alignments between the isoforms of β-tubulin were unambiguous due to the highly conserved amino acid sequences between these proteins. This alignment resulted in the filtering of both duplicates and fragmentary sequences and produced a final set of 23 unique sequences, from which eight distinct subtypes were classified, generally based on their overall amino acid sequence and specifically their carboxy terminal tail sequence.[23−27] Of the eight subtypes, βI (gi: 29788785) contained two additional isoforms (gi: 18088719, 338695). The βII isoform contained additional two sequences (gi: 4507729, 29788768) that carried differences in their carboxy terminal tail, however, class βIIa may actually correspond to a pseudogene.[23] In addition to the two βII tubulin genes, we also identified three additional proteins (gi: 27227551, 49456871, 7441369) that carry minor substitutions within the coding sequence. The βIII tubulin isoform (gi: 50592996) also contained two additional proteins (gi: 62897639, 1297274) which differ only by a single amino acid substitution. Two-class βIV tubulin genes (gi:21361322, 135470) differ only in their carboxy terminal tail sequences. The class βV (gi: 14210536) and βVI (gi: 62903515) are unique in their sequences. The class βVII tubulin gene family (gi: 55770868) contains additional two proteins (gi: 1857526, 12643363) that show slightly greater sequence variability than any of the other β-tubulin isoforms. Finally, the βVIII tubulin gene (gi: 42558279) is also unique in its sequence and has yet to be officially classified.[10]

The presence of both numerous tubulin structures and multiple tubulin isoform sequences offers a unique opportunity to apply homology modeling and create a library of human β-tubulin isoforms, from which we can determine their key biochemical characteristics. Following the solution of the three-dimensional structure of a protein, it becomes possible to use homology modeling to predict the structure of a protein that has a similar sequence.[28] Homology modeling utilizes several structural motifs from template proteins and pieces them together to form a final model. A scoring function assesses both the sequence identity between the target sequence and template and the overall quality of the template that is being considered. The scores are ranked and the fold with the best score is assumed to be the one adopted by the target sequence.[29] In this manner, we have

performed homology modeling on the complete set of human β-tubulin sequences.[9]

Currently, a total of five unique structures, upon which we can construct homology models of β-tubulin, are available in the Brookhaven Protein Databank. The first, and most obvious, choice was the initial structure of the α/β-tubulin heterodimer (PDB identifier 1TUB) proposed by Nogales et al.[30] However, this structure was produced at a comparatively low resolution and contains numerous omissions and misalignments due to difficulties in density fitting. A refinement of the 1TUB structure (PDB identifier 1JFF) was subsequently deposited with a slightly better resolution at 3.5 Å.[31] Along with increased resolution, the 1JFF structure also addressed a number of misalignment errors within the 1TUB structure and therefore makes a substantially better choice for a homology modeling template. Two additional structures of the tubulin heterodimer that are complexed with the stathmin-like domain, RB3-SLD, in the presence of colchicine (PDB identifier 1SA0) and vinblastine (PDB identifier 1Z20) are also available.[3,32] The 1SA0 structure was solved at 3.5 Å, while the 1Z20 structure was refined to only 4.1 Å. While the resolution of 1SA0 is slightly better than that in 1JFF, this structure contains a nine-residue gap in β-tubulin, ranging from Ser277 to Leu286. We chose to use both 1JFF and 1SA0 as our templates for modeling the human β-tubulin isoforms. Because the sequences within β-tubulin family are more similar to each other than to the other tubulin isoforms, it is reasonable to believe that any given sequence should produce a structure very similar to another member of a given family. Further support for this comes from the published structures of Nogales et al.[30] and Lowe et al.,[31] which are of a porcine sequence that were fit to structural data from an inhomogeneous bovine sample. Accordingly, by substituting appropriate amino acid side chains and properly adjusting other residues to accommodate insertions and deletions in the sequence, these crystallographic structures can be used as a framework to produce, with a high degree of confidence, model structures with different sequences.

To build the β-tubulin models we used Modeler (version 6v2),[33,34] which uses alignment of the sequences with known related structures, to obtain spatial restraints that the output structure must satisfy. Additional restraints derived from statistical studies of representative protein and chemical structures were also used to ensure a physically plausible result. Missing regions were predicted by simulated annealing using a molecular mechanics model. Although the Modeler program provides many options for model refinement and tuning, only the default parameters were used, as simple visual inspection of some of the output structures suggested that reasonable models were being produced. The quality of the resulting models was then investigated using two software packages: WHAT_CHECK[35] and PROCHECK.[36]

3. COLCHICINE BINDING SITE

Colchicine is a water-soluble alkaloid that, like paclitaxel, binds to α/β-tubulin dimers and blocks cell division thereby inhibiting mitosis. Unlike paclitaxel, the binding of colchicine does not result in microtubule stabilization but results in their destabilization. Initial structures of a two-heterodimer protofilament, complexed with the stathmin-like domain of RB3, were initially determined (PDB identifier 1FFX).[32] Recently, this work was followed by an additional structure that identified colchicine as binding between the α- and β-tubulin molecules within the heterodimer itself (PDB identifier 1SA0).[37] While the binding site for colchicine was shown to be at the interface between α- and β-tubulin, the majority of the interaction is actually restricted to the β-tubulin monomer. Ravelli et al. [37] identified several principal interactions between the bound colchicine and β-tubulin. First were interactions with strands S8 and S9, helix H7 and H8, and loop T7 (see ref 30). These interactions occur as a result of the colchicine binding site being buried within the intermediate domain of β-tubulin. The authors also suggest that interactions between colchicine and α-tubulin's T5 loop could result in the observed stabilization and bending of the heterodimer.[38] They also point out that upon binding of colchicine, the displacements of residues Asp249 and Lys349 are thought to interfere with filament formation. Additional biochemical data have also suggested that Val316 and Cys239 are also involved in colchicine binding.[39] Observations have also been made that suggest that the chemical sensitivity of Cys239 and Cys354, within β-tubulin, is altered upon binding of colchicine.[40]

Table 2. Tubulin Isoform Interactions with Colchicine

isoform	position		
βIII	Cys239-Ser	Ala315-Thr	Thr351-Val
βV	Cys239-Ser	Ala315-Thr	Thr351-Val
βVI	Val236-Ile Cys239-Ser	Ala315-Thr	Thr351-Val
βVII		Val255-Met Val313-Ala	
βVII		Val313-Ala	

We have identified a total of 29 residues of β-tubulin within the 6 Å cutoff range from the bound colchicine, namely: 235−240, 246−257, 312−316, and 347−352. Of these 29 residues, seven positions show differences between the β-tubulin isoforms. All of the observed substitutions occur within the H7 and H8 helix, as well as the S8 and S9 sheets. These positions were initially identified by Ravelli[37] as those that are displaced upon colchicine binding to β-tubulin. The differences here occur over a wide range of β-isoforms, encompassing βIII, βV, βVI, βVII, and βVIII (see Table 2 and Figure 1). Many of these substitutions are conservative, with the exception of the βVII position Val255-Met and the βIII, βVII, and βVII position Ala316-Thr/Cys. Interestingly, there are four positions within the tubulin sequence alignment that have no clear consensus residue over all the β-isoforms, one of which is position 316, which falls within the colchicine binding site and can accommodate either Val or Ile.

Furthermore, when comparing the results of our modeling of the colchicine binding site to the data obtained in the 1SA0 structure,[41] we see no obvious differences with the exception of Cys239-Ser in βIII, βV, and βVI. This was identified by Chaudhuri[40] as being involved with colchicine binding through cysteine labeling studies. This position, while spatially conserved, produces an altered chemical environment, the difference being the presence of a hydroxyl or sulfhydryl moiety. A change like this could be exploited by producing covalently bound forms of a drug, under certain conditions in the form of either a disulfide or ester linkage. Additionally, the substitution Val255-Met within the βVII

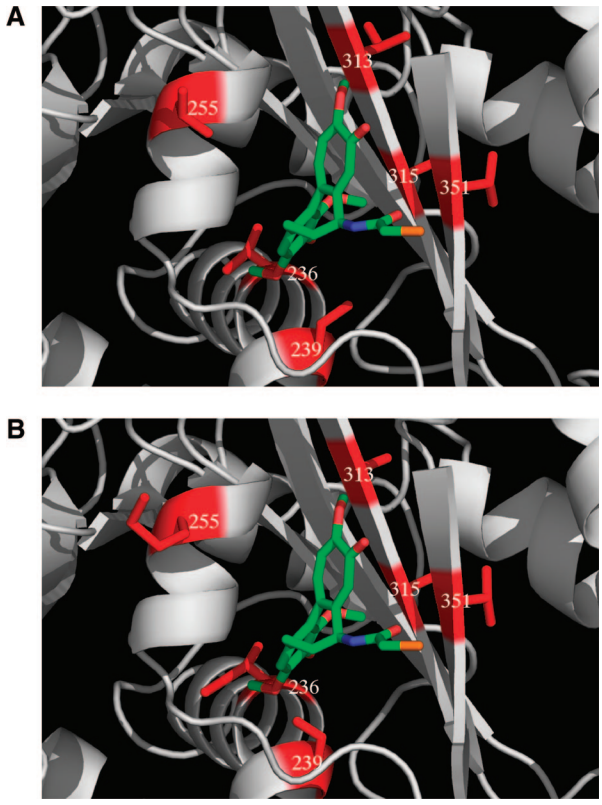

Figure 1. Schematic diagram of isoform differences in the colchicine binding site. Models of the βIII, βV, βVI, βVII, and βVIII isoforms were superimposed, along with the chain B from 1SA0,[32] and residues containing any atom within 6 Å of the bound colchicine molecule were selected. The amino side chain differences between each of the isoforms within this cutoff are shown as red sticks, while colchicine is shown as green sticks. (A) shows those residues, as they would be observed within the tubulin consensus sequence. (B) is an identical view as (A), with the exception that each position carries the appropriate amino acid substitution as seen in the isoforms.

isoform might alter the positional dynamics of helix H8 and therefore influence colchicine binding in this way. Residues that are present within the interface between H7/H8 and S8/S9, prior to their displacement upon colchicine binding, may also produce interactions that impart varied stability to this region.

Based upon this initial analysis of the 10 β-tubulin isoforms, it is clear that the greatest variability occurs within the sequences of βIII, βV, βVI, βVII, and βVIII. Interestingly, we see no variation, within the drug binding site, in βI, βII, or βIV. This may be due to conservation of the binding pocket structure, as a result of the importance of the underlying structure and dynamics of the microtubule. In addition to isoform specificity and drug binding analysis, recent experimental evidence has also suggested that microtubule dynamics can be changed by the inclusion of tubulin isoforms, in the absence of a bound drug molecule.[10] These results imply that when the equilibrium of microtubule assembly and disassembly is altered, the cell can respond by producing a specific tubulin isoform that will bring the system back to a normal balance. On the baasis of this hypothesis, we can also propose that the expression of tubulin isoforms that ultimately leads to microtubule destabilization may also play a role in the ability of cancerous cells to undergo rapid rounds of subsequent cell division.

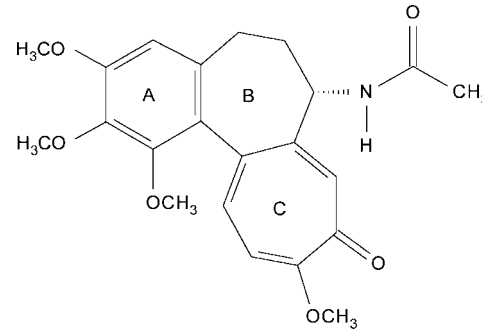

Figure 2. Structure of colchicine.

4. RELATIVE BINDING ENERGY CALCULATIONS

4.1. Setting up the Initial Structures. In forming the initial model for the α/β-tubulin heterodimer, only one type of α-tubulin subunit was used throughout the simulations and was taken from the RCSB Protein Data Bank with the PDB identifier 1SA0.[41] The 10 human β-tubulin isoforms used in the calculations were obtained from Huzil et al.[9,42] The α- and β-monomers were then joined together to form the 10 α/β-tubulin dimers. The coordinates of all the missing hydrogen atoms in the PDB structures were added using the DYNAMO[43] program. The geometry of each system was optimized by energy minimization to refine the structure as well as to relieve any bad contacts among atoms due to the creation of hydrogen atom coordinates.

The structure of colchicine is given in Figure 2. The two structural analogues of colchicine and the side groups used in this study are given in Figures 3 and 4, respectively. The modification to the first analogue is done by replacing the $-OCH_3$ in the C13 position of the A-ring of colchicine by different −OX groups. In the second analogue, the $-OCHX_3$ in the C11 position of the A-ring of colchicine is replaced by different −OY groups and the $-OCH_3$ in the C-ring is replaced by a $-SCH_3$. The molecular models for all the resulting derivative structures including colchicine were constructed using MOLDEN program.[44] The structures for each of these molecules were then optimized in the gas phase with the GAMESS-US[45] program using the AM1 semiempirical method.[46,47]

The geometry-optimized colchicine derivatives were positioned and oriented similarly to that of colchicine at the colchicine binding site between the α- and β-tubulin monomers. This procedure produced a total combination of 10 α/β-tubulin dimers × *n*-colchicine/derivatives systems. A suitable number of counterions were added to each colchicine/derivative−α/β-tubulin system to neutralize the charges on the tubulin dimer. Each system was then solvated by superimposing a rectangular box of water molecules with a dimension of 115 × 75 × 75 Å that was thermalized at 300 K. All water molecules overlapping with the atoms of the colchicine/derivative−α/β-tubulin system, and the counterions, with a buffer distance of 2.5 Å, were removed. Then, a geometry optimization was performed on each system using the conjugate-gradient method in DYNAMO to an rms gradient of 0.1 kJ/Å. Next, all water molecules beyond ∼7 Å from the surface of the α/β-tubulin complex were also deleted. This left about 30 000 atoms that included the α/β-tubulin, the colchicine/derivative, the counterions, and approximately two solvation layers of water surrounding the α/β-tubulin complex. A final geometry optimization was

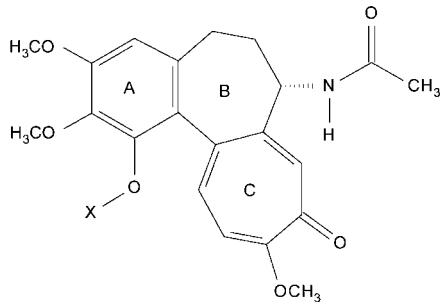

1	$-H$	**6**	$-CH_2CH_2CH_3$
2	$-COCH_3$	**7**	$-CH(CH_3)_2$
3	$-COCH_2CH_3$	**8**	$-CH_2CH(CH_3)_2$
4	$-COCH(CH_3)_2$	**9**	$-CH_2CH=CH_2$
5	$-CH_2CH_3$	**10**	$-CH_2CH_2OCH_3$

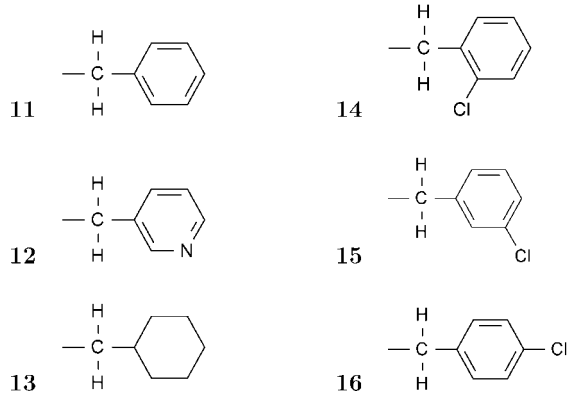

Figure 3. Structure of the colchicine analogue and the corresponding X-side groups.

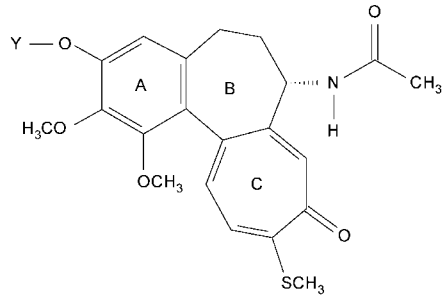

17	$-H$	**20**	$-CH_2CH_2CH_3$
18	$-CH_2CH=CH_2$	**21**	$-\alpha-D-glucose$
19	$-CH_2CH_3$	**22**	$-\beta-D-glucose$

Figure 4. Structure of the colchicine analogue and the corresponding Y-side groups.

performed on each system. All the residues within 18 Å of the colchicine/derivatives were then taken as the dynamically active part of the system while the rest were frozen. The division of the entire system into an active and a frozen part was used in all subsequent simulations.

Each of the individual colchicine and derivative molecules was also solvated in a manner similar to the procedure described above. The same rectangular box of water molecules was superimposed to each colchicine and derivative molecules. All water molecules overlapping with the atoms of the colchicine/derivatives and those beyond 30 Å were removed. The geometry of each system was optimized and partitioned into active and frozen parts similar to the colchicine/derivative−α/β-tubulin system described above.

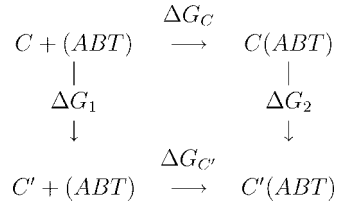

Figure 5. Thermodynamic cycle.

It should be noted that in all the geometry optimization steps performed, a hybrid quantum mechanical/molecular mechanical (QM/MM) approach was used. The QM/MM method was reviewed by Giao;[48] more recent developments were reported by Woodcock et al.[49] The colchicine and its derivatives were treated as QM atoms embedded within the MM atoms of the α/β-tubulin and water molecules. The AM1 semiempirical QM potential was used for the atoms of colchicine and derivatives while the OPLA-AA[50] force field was used as the potential for the tubulin atoms and TIP3P[51] for the atoms of water. In this QM/MM approach the active part interacted with the frozen part of the system.

4.2. Free Energy of Binding Calculations and Their Results. The thermodynamic cycle perturbation approach[52] shown in Figure 5 shows the scheme that is used as the basis for the determination of the free energies of binding. In this scheme, C and C′ represent colchicine and different modifications of colchicine, respectively, ABT represents the α/β-tubulin dimer, and the Δ*G*'s represent free energy changes for the indicated processes. The relative binding of C and C′ to ABT is determined by $\Delta\Delta G_{bind} = \Delta G_{C'} - \Delta G_C$. However, in practice, calculation of ΔG_C and $\Delta G_{C'}$ can be very difficult and challenging because the physical binding processes may involve conformational changes or even desolvation steps that are very slow. To overcome these difficulties, ΔG_1 and ΔG_2, although not physically measurable, are calculated instead via free energy perturbation using molecular dynamics. This is accomplished by performing simulations at different values of the perturbation parameter, λ. For example, the free energy difference between two states λ and $\lambda + \delta\lambda$ is calculated by using

$$\Delta G = G_{\lambda+\delta\lambda} - G_\lambda = -RT \ln\left\langle \exp\left(-\frac{(V_{\lambda+\delta\lambda} - V_\lambda)}{RT}\right)\right\rangle_\lambda \quad (1)$$

where $G_{\lambda+\delta\lambda}$ and G_λ are the respective free energies of state λ and $\lambda + \delta\lambda$, V_λ, and $V_{\lambda+\delta\lambda}$ are the potential energies both evaluated for the same configuration of the system, *R* is the gas constant, and *T* is the absolute temperature. The angle brackets denote the average value of the enclosed quantity for each configuration in the trajectory. The total free energy difference is calculated from the sum of the free energy differences of the related intermediate λ states:

$$\Delta G = \sum_{\lambda=0}^{\lambda=1} (G_{\lambda+\delta\lambda} - G_\lambda) \quad (2)$$

By using the thermodynamic cycle in Figure 5 and the fact that free energy is a state function, the relation, $\Delta\Delta G_{bind} = \Delta G_2 - \Delta G_1$, is justified.

In order to calculate the $\Delta\Delta G_{bind}$, two types of simulations were carried out—one for C and each C′, and another for the C(ABT) and each C′(ABT) noncovalent complex. In all the model structures, the initial coordinates were taken from

Table 3. Calculated Average $\Delta\Delta G_{bind}$ and Standard Deviations (in kcal/mol) for Colchicine Derivatives **1**−**16** against Colchicine in 10 α/β-Tubulin Dimers

derivative	I	IIA	IIB	III	IVA
1	−13.2 ± 1.8	5.9 ± 1.5	−2.8 ± 1.6	1.1 ± 1.7	5.5 ± 2.6
2	−9.6 ± 3.3	−24.8 ± 1.6	−7.9 ± 2.2	1.4 ± 2.2	15.1 ± 4.0
3	−19.9 ± 6.2	−10.7 ± 3.9	−17.0 ± 3.9	6.6 ± 2.4	−9.5 ± 4.7
4	−30.0 ± 4.8	−8.3 ± 2.1	−7.0 ± 3.9	2.2 ± 4.0	−8.2 ± 4.2
5	−13.8 ± 3.4	−11.5 ± 2.0	3.5 ± 2.4	5.0 ± 1.7	−7.0 ± 3.5
6	8.6 ± 4.0	4.8 ± 2.1	20.0 ± 1.7	−4.3 ± 1.3	8.1 ± 2.6
7	−2.8 ± 0.8	−9.8 ± 1.7	2.6 ± 1.7	1.2 ± 1.6	1.8 ± 2.3
8	−2.5 ± 2.7	−7.8 ± 1.6	1.1 ± 4.5	2.2 ± 3.0	3.5 ± 3.1
9	2.9 ± 5.8	−7.0 ± 1.9	0.1 ± 3.3	0.3 ± 4.4	14.1 ± 3.7
10	−10.6 ± 4.6	−13.2 ± 3.0	−4.9 ± 4.3	−21.7 ± 1.8	−15.9 ± 4.1
11	37.6 ± 1.6	−0.6 ± 0.8	10.7 ± 1.7	13.1 ± 0.3	3.2 ± 3.4
12	−15.6 ± 1.6	−23.2 ± 2.1	−4.1 ± 1.9	−15.1 ± 1.6	−2.8 ± 2.7
13	0.1 ± 2.3	−5.2 ± 3.4	9.7 ± 1.5	2.3 ± 2.2	−3.7 ± 2.3
14	−0.1 ± 4.0	−11.0 ± 1.9	0.6 ± 1.5	26.3 ± 1.9	26.5 ± 2.7
15	12.4 ± 3.3	−3.5 ± 1.6	−1.4 ± 0.8	6.3 ± 1.6	−4.3 ± 2.3
16	−2.8 ± 4.2	−3.9 ± 0.9	5.5 ± 1.8	−9.1 ± 3.8	−9.9 ± 3.5

derivative	IVB	V	VI	VII	VIII
1	−16.9 ± 2.7	−19.2 ± 1.0	−10.4 ± 2.9	2.1 ± 1.1	41.4 ± 3.3
2	−5.4 ± 3.9	−13.7 ± 2.9	−10.0 ± 2.2	7.5 ± 1.8	7.7 ± 1.7
3	−20.7 ± 7.6	−6.8 ± 3.5	−12.2 ± 6.5	−8.2 ± 3.3	7.7 ± 2.7
4	−10.0 ± 3.4	−8.3 ± 4.1	−27.9 ± 4.9	−6.7 ± 3.3	0.6 ± 2.4
5	−13.9 ± 2.1	−4.4 ± 3.3	−14.5 ± 3.4	6.7 ± 1.4	22.3 ± 2.2
6	−12.7 ± 5.7	10.8 ± 3.2	−3.9 ± 5.1	5.2 ± 2.3	21.2 ± 1.2
7	−10.2 ± 1.9	−12.7 ± 4.4	−2.2 ± 2.9	9.0 ± 1.3	16.0 ± 0.9
8	−16.5 ± 6.2	2.3 ± 2.5	−29.2 ± 5.4	−0.5 ± 3.8	12.6 ± 1.8
9	4.7 ± 6.3	−5.3 ± 4.1	−4.2 ± 6.0	16.1 ± 2.5	8.0 ± 2.2
10	−15.8 ± 6.1	−18.3 ± 4.2	−29.0 ± 6.5	−3.8 ± 3.7	6.8 ± 3.1
11	−19.1 ± 1.6	−4.2 ± 1.7	7.8 ± 4.2	10.6 ± 0.2	8.4 ± 1.4
12	−30.4 ± 3.3	−10.4 ± 4.8	−20.2 ± 3.5	30.3 ± 2.2	6.2 ± 0.8
13	−18.1 ± 3.6	1.1 ± 4.7	−11.3 ± 6.6	9.3 ± 4.7	12.8 ± 2.5
14	−20.0 ± 6.1	−2.0 ± 3.0	−16.2 ± 3.9	14.6 ± 2.8	37.9 ± 4.4
15	−4.4 ± 3.2	6.3 ± 2.0	−10.4 ± 3.2	7.4 ± 2.2	40.5 ± 1.1
16	−15.5 ± 2.2	−19.8 ± 2.3	−15.4 ± 2.6	8.7 ± 2.2	5.0 ± 0.9

Table 4. Calculated Average $\Delta\Delta G_{bind}$ and Standard Deviations (in kcal/mol) for Colchicine Derivatives **17**−**22** against Colchicine in 10 α/β-Tubulin Dimers

derivative	I	IIA	IIB	III	IVA
17	7.8 ± 5.1	−1.3 ± 1.4	3.1 ± 4.3	1.9 ± 1.5	26.1 ± 3.6
18	−2.1 ± 2.9	−1.1 ± 3.4	3.3 ± 2.8	16.8 ± 1.4	−5.6 ± 1.9
19	−10.3 ± 3.8	3.4 ± 3.2	−11.0 ± 2.3	−0.2 ± 1.5	−15.1 ± 3.2
20	−1.7 ± 5.1	0.9 ± 1.7	10.6 ± 3.5	7.8 ± 1.8	−6.4 ± 3.9
21	19.3 ± 4.6	25.2 ± 3.4	32.8 ± 2.9	38.0 ± 1.8	32.1 ± 2.4
22	−4.7 ± 4.8	−2.6 ± 2.5	−0.4 ± 4.4	23.8 ± 2.6	−1.9 ± 4.2

derivative	IVB	V	VI	VII	VIII
17	−6.6 ± 3.8	7.7 ± 2.0	−18.5 ± 5.9	23.9 ± 2.5	7.7 ± 2.9
18	−10.1 ± 2.3	−6.6 ± 3.1	−15.9 ± 5.1	−0.6 ± 1.3	9.9 ± 2.1
19	−6.1 ± 5.1	−12.9 ± 4.2	−33.6 ± 3.4	4.4 ± 2.4	6.6 ± 1.4
20	−8.4 ± 3.7	4.8 ± 2.9	−16.2 ± 4.9	11.0 ± 3.2	11.3 ± 1.4
21	27.3 ± 3.8	21.3 ± 3.0	11.8 ± 5.7	48.8 ± 4.1	50.9 ± 2.5
22	2.2 ± 3.2	15.8 ± 2.7	−9.2 ± 7.0	21.2 ± 5.0	8.1 ± 2.8

the final step of the structure preparation described above. In all the simulations, prior to the start of free energy perturbation calculations, each system was energy minimized using a conjugate-gradient method to an rms gradient of 0.1 kJ/Å, and then equilibrated for 10 ps at 300 K with molecular dynamics. In order to control the temperature and approximate a canonical ensemble, all molecular dynamics simulations were done with a Langevin algorithm using a friction coefficient of 10^{-1} ps for each atom and a time step of 1 fs. The QM/MM and MM/MM nonbonding interactions were calculated using an atom-based force-switching truncation function with inner and outer cutoffs of 9.0 and 13.0 Å, respectively, and a nonbonded cutoff of 15.0 Å. The QM charges of colchicine and its derivatives in the last step of the equilibration were then saved and used in the subsequent classical free energy perturbation calculations. Since there are interactions among QM and MM atoms, we chose to use these calculated QM charges for the colchicine/derivatives in the presence of MM charges, as opposed to just QM charges calculated in the gas phase (i.e., the influence of MM charges in calculating QM charges is taken into account). We believe that these calculated QM charges are a better representation of actual charges that can be used in the classical free energy perturbation calculations described next.

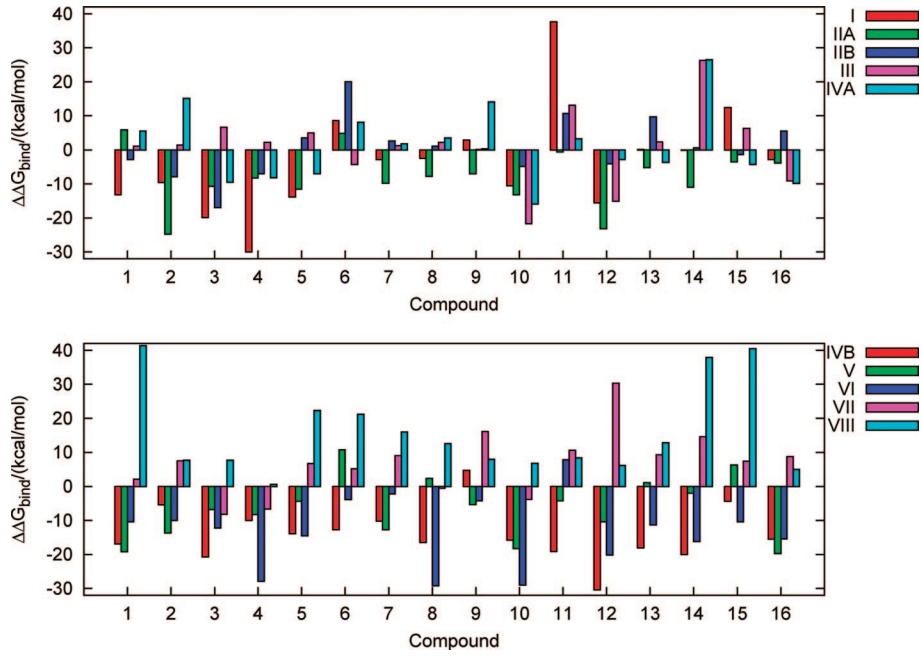

Figure 6. α/β-Tubulin isoforms and compounds **1**−**16**.

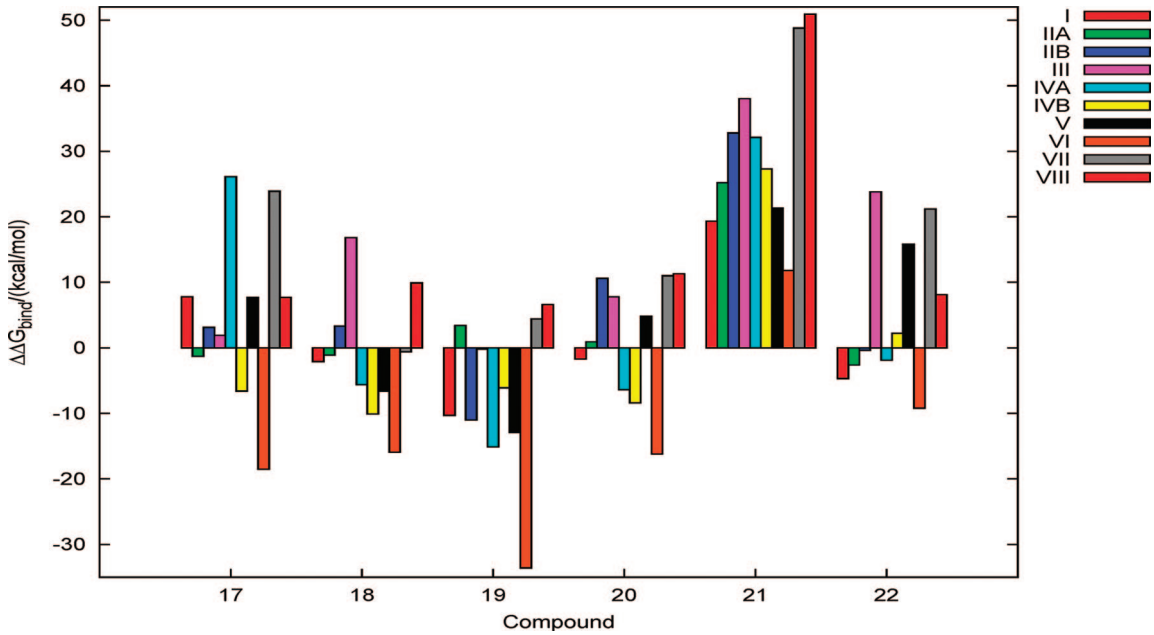

Figure 7. α/β-Tubulin Isoforms and Compounds **17**−**22**.

Other schemes for deriving partial atomic charges, such as CHELP, CHELPG, Merz−Kollman, and RESP, can also be used.[53]

For the classical free energy perturbation calculations, the electrostatic free energy was evaluated separately from the van der Waals energy. For a smooth evaluation of the van der Waals free energies, only the van der Waals well depth was explicitly changed in each step of the perturbation calculations. At the beginning of each simulation, we used the coordinates from the last step of the equilibration described above. The perturbation was immediately performed with varying time lengths of 1.0, 1.5, 2.0, and 2.5 ps for each of the equilibration and data collection steps, using a 1 fs time step. Both the forward ($\lambda = 1 \rightarrow 0$) and backward ($\lambda = 0 \rightarrow 1$) changes in the free energies were evaluated. At each window of equilibration and data collection, λ was varied by 0.05. The average binding free energies and the standard deviations were then calculated from these four free energy perturbation calculations. All molecular dynamics and free energy perturbation calculations are done using DYNAMO.

Tables 3 and 4 show the calculated changes in the binding free energies with respect to colchicine which was used as a reference point for all the molecules shown in Figures 3 and 4, respectively. Figures 6 and 7 give a visual representation of the ranking of the analogues when used as a replacement for colchicine for the 10 α/β-tubulin isoforms that were used in the study. The $\Delta\Delta G_{bind}$ with negative values correspond to molecules that are more strongly bound to the α/β-tubulin dimers than colchicine, while those with positive values correspond to those that are less strongly bound to them. The results of the simulations indicate that

there are compounds that potentially could be superior substitutes for colchicine. In Figure 6, compound **10** exhibits the best among the compounds studied as it shows that it is more strongly bound to all isoforms with respect to colchicine except with its binding with α/βVIII. In Figure 7, compound **19** shows the best binding to 7 out of 10 α/β-tubulin isoforms.

As can be seen from Figures 6 and 7, the relative binding energy with respect to colchicine is selective. None of the derivatives exhibits the best or worst binding overall, with the sole exception of compound **21**, that does so in all the 10 α/β-tubulin dimers. This variability is expected and can be attributed to the differences in the amino acid side chains within the colchicine binding site of the 10 α/β-tubulin dimers.

5. CONCLUSION

The estimated values of $\Delta\Delta G_{\text{bind}}$ presented in this paper can serve as a first of the many steps in designing, testing, and identifying specific chemotherapeutic compounds for targeting specific tubulin isoforms that are overexpressed in cancer cells. The ultimate goal of cancer research is to develop a drug or treatment regimen that will target only cancer cells and will target them absolutely. The significance of microtubules as a target for chemotherapeutic treatments is outlined in a recent review by Jordan and Wilson.[54] They emphasize the importance of understanding the underlying mechanistic processes of these drugs when they bind to the target protein. While it is clear that a substantial amount of experimental work has to be done on obtaining kinetic data for drug binding to each β-tubulin isoform, the presence of minor variations within the structure of β-tubulin isoforms may provide us with an initial starting point for the development of novel drugs, or the derivatization of existing drugs that have increased specificity. This paper provided an attempt in this direction by investigating a diversity within a specific group of colchicine derivatives. We are encouraged by the results showing a degree of specificity for each tubulin isoform exhibited by the panel of the designed colchicine derivatives. We expect that these results will be supported by in vitro experiments. This type of approach, when brought to a successful completion, may eventually allow us to develop secondary treatments for cancer cell lines that have developed drug resistance, due to mutations or altered expression levels, as a result of standard chemotherapy treatments.

We are aware of the existence of various mutations affecting the amino acid sequence of β-tubulin. Many of these mutations are somatic and develop within the tumor site. A number of common mutations have been identified to occur in the colchicine binding site and they may lead to the development of drug resistence over the course of chemotherapy. To overcome this complication, we intend to calculate the binding affinities of these tubulin mutants for the colchicine derivatives discussed in this paper and select the optimized structures for the particular overexpressed mutant which could eventually result in better cure outcomes.

ACKNOWLEDGMENT

All the calculations were done on the IBM RS/6000 workstations and on the General Purpose Linux cluster (Academic Information and Communication Technology) at the University of Alberta, as well as on the computers of WestGrid. The present work was funded in part by a research grant from MITACS and NSERC. We also thank The Allard Foundation, Oncovista, LLC of San Antonio, TX, and Technology Innovations, LLC of Rochester, NY, for additional support.

REFERENCES AND NOTES

(1) Mitchison, T.; Kirschner, M. Dynamic instability of microtubule growth. *Nature* **1984**, *312*, 237–242.
(2) Toso, R.; Jordan, M.; Farrell, K.; Matsumoto, B.; Wilson, L. Kinetic stabilization of microtubule dynamic instability in vitro by vinblastine. *Biochemistry* **1993**, *32*, 1285–1293.
(3) Gigant, B.; Wang, C.; Ravelli, R.; Roussi, F.; Steinmetz, M.; Curmi, P.; Sobel, A.; Knossow, M. Structural basis for the regulation of tubulin by vinblastine. *Nature* **2005**, *435*, 519–522.
(4) Zagrovic, B.; van Gunsteren, W. F. Computational analysis of the mechanism and thermodynamics of inhibition of phosphodiesterase 5A by synthetic ligands. *J. Chem. Theory Comput.* **2007**, *3*, 301–311.
(5) Klauda, J. B.; Brooks, B. R. Sugar binding in lactose permease: Anomeric state of a disaccharide influences binding structure. *J. Mol. Biol.* **2007**, *367*, 1523–1534.
(6) Bren, M.; Florian, J.; Mavri, J.; Bren, U. Do all pieces make a whole? Thiele cumulants and the free energy decomposition. *Theor. Chem. Acc.* **2007**, *117*, 535–540.
(7) Hamel, E. *Microtubule Proteins*; CRC Press: Boca Raton, FL, 1990.
(8) Wilson, L.; Jordan, M. *Microtubules*; Wiley-Liss: New York, 1994.
(9) Huzil, J.; Luduena, R.; Tuszynski, J. Comparative modelling of human β tubulin isotypes and implications for drug binding. *Nanotechnology* **2006**, *17*, S90–S100.
(10) Panda, D.; Miller, H.; Banerjee, A.; Luduena, R.; Wilson, L. Microtubule dynamics in vitro are regulated by the tubulin isotype composition. *Proc. Natl. Acad. Sci. U.S.A.* **1994**, *91*, 11358–11362.
(11) Banerjee, A.; Kasmala, L. Differential assembly kinetics of α-tubulin isoforms in the presence of paclitaxel. *Biochem. Biophys. Res. Commun.* **1998**, *245*, 349–351.
(12) Sept, D.; Baker, N.; McCammon, J. The physical basis of microtubule structure and stability. *Protein Sci.* **2003**, *12*, 2257–2261.
(13) Ranganathan, S.; Dexter, D.; Benetatos, C.; Chapman, A.; Tew, K.; Hudes, G. Increase of βIII- and βIVa-tubulin isotopes in human prostate carcinoma cells as a result of estramustine resistance. *Cancer Res.* **1996**, *56*, 2584–2589.
(14) Liu, B.; Staren, E.; Iwamura, T.; Appert, H.; Howard, J. Mechanisms of taxotere-related drug resistance in pancreatic carcinoma. *J. Surg. Res.* **2001**, *99*, 179–186.
(15) Hari, M.; Yang, H.; Zeng, C.; Canizales, M.; Cabral, F. Expression of class III β-tubulin reduces microtubule assembly and confers resistance to paclitaxel. *Cell Motil. Cytoskeleton* **2003**, *56*, 45–56.
(16) Mozzetti, S.; Ferlini, C.; Concolino, P.; Filippetti, F.; Raspaglio, G.; Prislei, S.; Gallo, D.; Martinelli, E.; Ranelletti, F.; Ferrandina, G.; Scambia, G. Class III β-tubulin overexpression is a prominent mechanism of paclitaxel resistance in ovarian cancer patients. *Clin. Cancer Res.* **2005**, *11*, 298–305.
(17) Khan, I.; Luduena, R. Different effects of vinblastine on the polymerization of isotypically purified tubulins from bovine brain. *Invest. New Drugs* **2003**, *21*, 3–13.
(18) Banerjee, A.; Luduena, R. Kinetics of colchicine binding to purified β-tubulin isotypes from bovine brain. *J. Biol. Chem.* **1992**, *267*, 13335–13339.
(19) Hardman, J.; Limbird, L. *Goodman & Gilman's The Pharmaco-logical basis of therapeutics*, 9th ed.; McGraw-Hill: New York, 1996.
(20) Scott, C.; Walker, C.; Neal, D.; Harper, C.; Bloodgood, R.; Somers, K.; Mills, S.; Rebhun, L.; Levine, P. β-tubulin epitope expression in normal and malignant epithelial cells. *Arch. Otolaryngol. Head Neck Surg.* **1990**, *116*, 583–589.
(21) Apweiler, R.; Bairoch, A.; Wu, C.; Barker, W.; Boeckmann, B.; Ferro, S.; Gasteiger, E.; Huang, H.; Lopez, R.; Magrane, M.; Martin, M.; Natale, D.; O'Donovan, C.; Redaschi, N.; Yeh, L. UniProt: The universal protein knowledgebase. *Nucleic Acids Res.* **2004**, *32*, D115–D119.
(22) Thompson, J.; Higgins, D.; Gibson, T. CLUSTAL W: Improving the sensitivity of progressive multiple sequence alignment through sequence weighting, position-specific gap penalties and weight matrix choice. *Nucleic Acids Res.* **1994**, *22*, 4673–4680.
(23) Lee, M.; Lewis, S.; Wilde, C.; Cowan, N. Evolutionary history of a multigene family: An expressed human β-tubulin gene and three processed pseudogenes. *Cell* **1983**, *33*, 477–487.
(24) Hall, J.; Dudley, L.; Dobner, P.; Lewis, S.; Cowan, N. Identification of two human β-tubulin isotypes. *Mol. Cell. Biol.* **1983**, *3*, 854–862.

(25) Lewis, S.; Gilmartin, M.; Hall, J.; Cowan, N. Three expressed sequences within the human β-tubulin multigene family each define a distinct isotype. *J. Mol. Biol.* **1985**, *182*, 11–20.
(26) Burgoyne, R. D.; Cambray-Deakin, M.; Lewis, S.; Sarkar, S.; Cowan, N. Differential distribution of β-tubulin isotypes in cerebellum. *EMBO J.* **1988**, *7*, 2311–2319.
(27) Strausberg, R. Mammalian Gene Collection Program Team. Generation and initial analysis of more than 15,000 full-length human and mouse cDNA sequences. *Proc. Natl. Acad. Sci. U.S.A.* **2002**, *99*, 16899–16903.
(28) Chothia, C.; Lesk, A. The relation between the divergence of sequence and structure in proteins. *EMBO J.* **1986**, *5*, 823–826.
(29) Luthy, R.; Bowie, J.; Eisenberg, D. Assessment of protein models with three-dimensional profiles. *Nature* **1992**, *356*, 83–85.
(30) Nogales, E.; Wolf, S.; Downing, K. Structure of the α/β tubulin dimer by electron crystallography. *Nature* **1998**, *391*, 199–203.
(31) Lowe, J.; Li, H.; Downing, K.; Nogales, E. Refined structure of α/β at 3.5 Å resolution. *J. Mol. Biol.* **2001**, *313*, 1045–1057.
(32) Gigant, B.; Curmi, P.; Martin-Barbey, C.; Charbaut, E.; Lachkar, S.; Lebeau, L.; Siavoshian, S.; Sobel, A.; Knossow, M. The 4 Å X-ray structure of a tubulin:stathmin-like domain complex. *Cell* **2000**, *102*, 809–816.
(33) Sali, A.; Blundell, T. Comparative protein modelling by satisfaction of spatial restraints. *J. Mol. Biol.* **1993**, *234*, 779–815.
(34) Sanchez, R.; Sali, A. Comparative protein structure modeling: Introduction and practical examples with Modeller. *Methods Mol. Biol.* **2000**, *143*, 97–129.
(35) Hooft, R.; Vriend, G.; Sander, C.; Abola, E. Errors in protein structures. *Nature* **1996**, *381*, 272.
(36) Laskowski, R.; MacArthur, M.; Moss, D.; Thornton, J. Procheck: A program to check the stereochemical quality of protein structures. *J. Appl. Crystallogr.* **1993**, *26*, 283–291.
(37) Ravelli, R.; Gigant, B.; Curmi, P.; Jourdain, I.; Lachkar, S.; Sobel, A.; Knossow, M. Insight into tubulin regulation from a complex with colchicine and a stathmin-like domain. *Nature* **2004**, *428*, 198–202.
(38) Luduena, R.; Roach, M. Tubulin sulfhydryl groups as probes and targets for antimitotic and antimicrotubule agents. *Pharmacol. Ther.* **1991**, *49*, 133–152.
(39) Bai, R.; Covell, D.; Pei, X.; Ewell, J.; Nguyen, N.; Brossi, A.; Hamel, E. Mapping the binding site of colchicinoids on β-tubulin: 2-chloroacetyl-2-demethylthiocolchicine covalently reacts predominantly with cysteine 239 and secondarily with cysteine 354. *J. Biol. Chem.* **2000**, *275*, 40443–40452.
(40) Chaudhuri, A.; Seetharamalu, P.; Schwarz, P.; Hausheer, F.; Luduena, R. The interaction of the B-ring of colchicine with α-tubulin: A novel footprinting approach. *J. Mol. Biol.* **2000**, *303*, 679–692.
(41) Ravelli, R.; Gigant, B.; Curmi, P.; Jourdain, I.; Lachkar, S.; Sobel, A.; Knossow, M. Insight into tubulin regulation from a complex with colchicine and a stathmin-like domain. *Nature* **2004**, *428*, 198–202.
(42) Huzil, J.; Chen, K.; Kurgan, L.; Tuszynski, J. The roles of β- tubulin mutations and isotype expression in acquired drug resistance. *Cancer Informatics* **2007**, *3*, 159–181.
(43) Field, M. J.; Albe, M.; Bret, C.; Martin, F.; Thomas, A. The DYNAMO library for molecular simulations using hybrid quantum mechanical and molecular mechanical potentials. *J. Comput. Chem.* **2000**, *21*, 1088–1100.
(44) Schaftenaar, G.; Noordik, J. Molden: A pre- and post-processing program for molecular and electronic structures. *J. Comput.-Aided Mol. Des.* **2000**, *14*, 123–134.
(45) Schmidt, M. W.; Baldridge, K. K.; Boatz, J. A.; Elbert, S. T.; Gordon, M. S.; Jensen, J. H.; Koseki, S.; Matsunaga, N.; Nguyen, K. A.; Su, S.; Windus, T. L.; Dupuis, M.; Montgomery, J. A. General atomic and molecular electronic structure system. *J. Comput. Chem.* **1993**, *14*, 1347–1363.
(46) Dewar, M.; Zoebisch, E.; Healy, E.; Stewart, J. AM1: A new general purpose quantum mechanical molecular model. *J. Am. Chem. Soc.* **1985**, *107*, 3902–3909.
(47) Dewar, M.; Dieter, K. Evaluation of AM1 calculated proton affinities and deprotonation enthalpies. *J. Am. Chem. Soc.* **1986**, *108*, 8075–8086.
(48) Giao, J. Methods and applications of combined quantum mechanical and molecular mechanical potentials. *Rev. Comput. Chem.* **1996**, *7*, 119–185.
(49) Woodcock, H. L.; Hodošček, M.; Brooks, B. R. Exploring SCC-DFTB paths for mapping QM/MM reaction mechanisms. *J. Phys. Chem. A* **2007**, *111*, 5720–5728.
(50) Jorgensen, W.; Maxwell, D.; Tirado-Rives, J. Development and testing of the OPLS all-atom force field on conformational energetics and properties of organic liquids. *J. Am. Chem. Soc.* **1996**, *118*, 11225–11236.
(51) Jorgensen, W.; Chandrasekhar, J.; Madura, J.; Impey, R.; Klein, M. Comparison of simple potential functions for simulating liquid water. *J. Chem. Phys.* **1983**, *79*, 926–935.
(52) Tembe, B.; McCammon, J. Ligand-receptor interactions. *Comput. Chem.* **1984**, *8*, 281–283.
(53) Sigfridsson, E.; Ryde, U. Comparison of methods for deriving atomic charges from the electrostatic potential and moments. *J. Comput. Chem.* **1998**, *19*, 377–395.
(54) Jordan, M.; Wilson, L. Microtubules as a target for anticancer drugs. *Nat. Rev. Cancer* **2004**, *4*, 253–265.

CI800054N